North American boreal forests are a large carbon source due to wildfires from 1986 to 2016

Bailu Zhao
Purdue University https://orcid.org/0000-0002-1326-4801
Qianlai Zhuang (qzhuang@purdue.edu)
Purdue University West Lafayette https://orcid.org/0000-0002-4536-9851
Narasinha Shurpali
Natural Resources Institute Finland (Luke)
Kajar Köster
Estonian Young Academy of Sciences
Frank Berninger
University of Eastern Finland
Jukka Pumpanen
University of Eastern Finland

Article

Keywords: Forest Carbon Balance, Biogeochemistry Model, Wildfires

Posted Date: September 18th, 2020

DOI: https://doi.org/10.21203/rs.3.rs-73841/v1

North American boreal forests are a large carbon source due to wildfires from 1986 to 2016

Bailu Zhao[1], Qianlai Zhuang[1,2], Narasinha Shurpali[3], Kajar Köster[4], Frank Berninger[5], Jukka Pumpanen[6]

[1]Department of Earth, Atmospheric, and Planetary Sciences, Purdue University, West Lafayette, Indiana, 47907
[2]Department of Agronomy, Purdue University, West Lafayette, IN 47907
[3]Natural Resources Institute Finland (Luke)
[4]Department of Forest Sciences, University of Helsinki, PO Box 27, FI-00014 University of Helsinki, Finland
[5]Department of Environmental and Biological Sciences, University of Eastern Finland, PO Box 111, FI-80101 Joensuu, Finland
[6]Department of Environmental and Biological Sciences, University of Eastern Finland, PO Box 1627, FI-70211 Kuopio, Finland
* Correspondence to: qzhuang@purdue.edu

Abstract

Wildfires are a major disturbance to forest carbon (C) balance through both immediate combustion emissions and post-fire ecosystem dynamics. Here we use a process-based biogeochemistry model, the Terrestrial Ecosystem Model (TEM), to simulate C budget in Alaska and Canada during 1986-2016, as impacted by fire disturbances. We extracted the data of difference Normalized Burn Ratio (dNBR) for fires from Landsat TM/ETM imagery and estimated the proportion of vegetation and soil C combustion. We observed that the region is a C source of 2.74 Pg C during the 31-year period. The observed C loss, 57.1 Tg C yr^{-1}, was attributed to fire emissions, overwhelming the net ecosystem production (1.9 Tg C yr^{-1}) in the region. Our simulated during-fire emissions for Alaska and Canada are within the range of field measurements and other model estimates. As burn severity increases, combustion emission tended to switch from vegetation origin towards soil origin. Burn severity regulates post-fire C dynamics. Low severity fires increase soil temperature and decrease soil moisture and thus, enhance soil respiration. However, the opposite trend was found under moderate or high burn severity. The proportion of post-fire soil emission in total emissions increased with burn severity. Net nitrogen mineralization gradually recovered after fire, enhancing net primary production. Net ecosystem production recovered fast under higher burn severities. The impact of fire disturbance on the C balance of northern ecosystems and the associated uncertainties can be better characterized with long-term, prior, during- and post-disturbance data across the geospatial spectrum. Our findings suggest that the regional source of carbon to the atmosphere will persist if the observed forest wildfire occurrence and severity continues into the future.

Introduction

Boreal forests become more important in the global carbon (C) cycling as the climate gets warmer. These ecosystems store one-third of the global terrestrial C Kasischke and Stocks [1] and prevalent wildfires accelerate their C release into the atmosphere [2]. Massive amounts of C are released directly through biomass combustion.

Post-fire C dynamics leading to increased heterotrophic respiration (R_H) and decreased net primary production contribute to the C loss, shifting boreal forests from a C sink to a source [3]. Previous studies have shown that wildfires also significantly increased global land annual mean surface temperature in the 20th century by 0.18 °C [4]. The warmer climate resulting from anthropogenic greenhouse gases and aerosol emissions has caused larger burned area in Canadian forests [5]. Within the last four decades, twice larger burned area and twice higher frequency of large fire events (> 1000 km^2) in Canada have been reported [6]. These observational studies indicate that there is a positive feedback between wildfires and the global climate.

Wildfires influence the C dynamics in the boreal forests of North America (NA) primarily through removing aboveground vegetation, since the regional forest species are susceptible to crown fires [7,8]. After severe fires, forests could temporarily shift to grasslands [9]. Alternatively, in response to the changes in temperature and moisture conditions as well as soil organic layer thickness, the newly-emerged dominant tree species might be different from the pre-fire community [10-12]. In either case, following the reduction of leaf area after the fire, the mass and energy fluxes between the biosphere and atmosphere will change, further influencing soil moisture, temperature and C dynamics [4,9,13].

Wildfires also dramatically affect soil C storage and ecosystem C balance [14,15]. Soil organic matter combustion could release massive amounts of C to the atmosphere in severe fires. Nearly 90% of total combusted C in a North American boreal fire in 2014 was from soils (e.g., ref [16]). Together with immediate fire emissions from soils, the post-fire soil C emissions through soil respiration could further imbalance the C budget. The soil respiration is determined by soil thermal and moisture conditions and microbial community, which are all altered by fire [17]. Fires result in higher thermal conductivity in the ground and lower albedo by removing plant tissues and the organic layer on the surface [4,18,19]. This would increase soil temperature due to increasing solar radiation on the soil surface after the fire [13,20]. Soil water conditions after the fire will depend on the severity of fire because the density of trees and ground vegetation determines the ecosystem evapotranspiration and the overland water flow [21]. For example, no soil moisture change was observed in a less severely burned forest in central Colorado in 2002, while a severely burned forest in this region had high soil moisture [20]. The shift in dominant microbial members, lower soil moisture and C storage collectively affect long-term post-fire CO_2 emissions [22]. For example, soil CO_2 efflux would initially reduce and then increase for several decades [23], mainly due to the dynamics of soil C and fungi biomass recovery after the fire [24].

Although the influence of fire on the boreal C budget has been previously modeled [2,25-27], several limitations in these studies are evident. First, fire-induced CO_2 emissions in many boreal regions, such as Russia [25,28], Alaska [27], Canada [29] and the Northern Hemisphere as a whole [30] have primarily focused on immediate combustion emission estimates. However, long-term post-fire soil emissions and NPP changes could account for a large proportion of total fire-related C loss [29]. Second, for both during- and post-fire C emissions, a few site-level studies are conducted based on field measurements [16,22,24]. At the regional scale, process-based models are necessary when site-level observations are limited [26]. Third, although burn severity is an important control of C

emissions, regional estimations are rare and records are limited [25]. Burn severity can be expressed as the fraction [31] or amount [25] of pre-fire ecosystem C lost during the fire. Unfortunately, burn severity information is not available in existing fire datasets (AICC, CWFIS, see *SI* and methods for details). When estimating regional C combustion, an average severity is generally assumed for an entire region [26,27,30] or biome type [32]. These severity estimates are based on data published in the literature, limited available field data or expert knowledge, while the actual burn severity could differ dramatically among fires [33].

To overcome these limitations mentioned above, we applied a process-based model, the Terrestrial Ecosystem Model (TEM; [34]), to understand the role of fire disturbance on the C budget of North American boreal forests using burn severity data retrieved from satellite images. Difference Normalized Burn Ratio (dNBR) from LANDSAT imagery was used to represent burn severity, which was used to estimate the proportion of vegetation and soil removal by fire. We have thus extracted burn severity information for all fires during 1986-2016. We conducted regional simulations for the study period and evaluated the spatial and temporal C dynamics considering fire impacts on C emissions, soil physics, soil nutrient status, and the subsequent net ecosystem production. Different from previous modelling studies, this study is scaling up of burn severity indices for all fires during the study period. We hypothesize that the during- and post-fire influences on the vegetation and soil and resultant C and N dynamics vary depending upon the burn severity.

Results

Fire regime during 1986-2016. Although the average fire interval in boreal forests is 80 years [35], the areas burned more than once in the 31-year period of 1986-2016 still account for 4.8% of the total burned area. During this period, the number of fires generally increased, while the annual burned area didn't show an increasing trend despite a large amplitude (the difference between the largest and smallest burned areas) (Fig. 1a). For most of the burned areas, the average dNBR value was 200-400, with an overall area-weighted average of 272.52 (Fig. 1b). Although the dNBR varied greatly within a year, annual area-weighted dNBR significantly increased during the 31-year period (Fig. 1c). The trend is expressed as:

$$dNBR = 3.14 \times year - 6014.54 \ (R^2 = 0.33, P < 0.001) \quad (1)$$

Spatial patterns of fire impacts on ecosystem C balance. The spatial pattern of C emissions during combustion followed that of the fire area and severity (Fig. 2 & Fig. 3a). In particular, the total combustion emissions of the North American boreal forests during 1986-2016 were 1769.8 Tg, with hotpots in Saskatchewan and Quebec, Canada. When no fire disturbance was considered, the majority of forests acted as C sinks, with a total 31-year cumulative NEP of 1030.0 Tg. In addition, C sequestration in these forests was higher in the east than in the west (Fig. 3b). The spatial pattern of cumulative NEP under fire also followed the fire distribution pattern, since fires removed vegetation and soil C and reduced NPP (Fig. 3c). Although fire greatly reduces the productivity of boreal forests, the 31-year regional cumulative NEP was still positive (59.0 Tg). Meanwhile, the spatial pattern of the difference between fire and no-fire NEP had a similar spatial pattern to fire events (Fig. 3d). In addition, spatial patterns of total C stocks were the same as

NEP (Fig. 3b), since it is the difference between NEP (59.0 Tg) and combustion emissions (1769.8 Tg). Therefore, although the NA boreal forests showed signs of recovery with a positive regional cumulative NEP during the study period, they acted as a C source (Fig. 3e). Due to massive fire emissions and reduced post-fire productivity, the total ecosystem C stocks were reduced by 2740.8 Tg during the 31-year period compared with the estimate without fires. The pattern of differences between the C stocks with and without fires was highly consistent with that of the fire emission (Fig. 3f).

Temporal pattern of fire impacts on ecosystem C balance. Fire area rather than the number of wildfire occurrences controls the spatial fire emission patterns (Supplementary Fig. 1a & Fig. 3a). When fires were not taken into account, the simulated regional forest biomass and soil organic C stocks increased from 1986 to 2016, while an opposite trend was found when fire impacts were taken into account (vegetation C: 557.0 Tg for no-fire vs -468.9 Tg for fire, soil organic C: 589.5 Tg for no fire vs -1125.4 Tg for fire, Supplementary Fig. 1a & c). Although the mean burn severity increased during the study period (Fig. 1c), the combustion emissions did not show such a trend due to a wide variation in the burned area. With and without fires, the estimated annual regional NPP, R_H and their difference, i.e. NEP, highly varied and were generally synchronous with each other (Supplementary Fig. 1e & f). When fires were taken into account in the simulation, NPP was always lower than that without fires, and their differences increased with year over the study period (Supplementary Fig. 1g). This was attributed to the removal of plant biomass due to fires. The difference in vegetation C storage (proportional to vegetation biomass) between the two scenarios grew larger with time (Supplementary Fig. 1b). The relationship between NPP difference and year (ranges between 1986 and 2016) is:

$$NPP_{diff} = 0.0014 \times year - 2.85 \ (R^2 = 0.66, P < 0.001) \quad (2)$$

In contrast, R_H with fire regimes considered was generally higher before 2000, and similar in the early 2000s, suggesting that, despite the lower soil organic C storage with fires, other factors (e.g., soil temperature and moisture) might stimulate soil respiration. However, since the latter 2000s, R_H decreased with fires because the reduced soil organic C overrode the effect of soil temperature and moisture changes (Supplementary Fig. 1c & h). The relationship between year and R_H difference is:

$$Rh_{diff} = 1.86 \times 10^{-5} \times year^2 - 0.074 \times year + 74.07 \ (R^2 = 0.87, P < 0.001) \quad (3)$$

The trend in NEP differences between fires and no-fires was more consistent with the difference in NPP than in R_H since NPP was larger in magnitude (Supplementary Fig. 1i). By 2016, fires resulted in a lower cumulative NEP by 971.0 Tg than the no-fire scenario in the region. The relationship between the year and the NEP difference is:

$$NEP_{diff} = 0.0012 \times year - 2.35 \ (R^2 = 0.53, P < 0.001) \quad (4)$$

Influence of burn severity. According to the dNBR values, burn severity was classified into seven levels with an interval of 100 for comparison (Fig. 4). On average, wildfires removed 1512.0 g C m^{-2} of vegetation C in the region, with higher burn severity leading to higher removal rate (ranging between 1382.3-1951.4 g C m^{-2}, Fig. 4a). Vegetation growth recovered steadily following fires, and by the 25th year, the difference in vegetation C between the fire and no-fire scenarios decreased to 773.0-1242.2 g C m^{-2}.

Net nitrogen (N) mineralization decreased on average by 1401.1 g N $m^{-2} \cdot yr^{-1}$ in the year of fire. Since the second year after the fire, the net N mineralization rate had increased and recovered by 1066.5 N $yr^{-1} \cdot m^{-2}$ by the 25th year after fire (Fig. 4b). Similarly, the productivity of vegetation was reduced by 170.5 g C $yr^{-1} \cdot m^{-2}$ in the year of fire. However, after the fire, NPP increased regardless of burn severity with the subsequent vegetation regrowth. In the 25th year after the fire, the NPP difference between the two scenarios reduced by 132.6 g C $yr^{-1} \cdot m^{-2}$ (Fig. 4c).

Fire removed 499.1 g C m^{-2} of soil organic C. Compared with vegetation C, the removal of soil organic C showed more variations (ranging between 116.1-5057.1 g C m^{-2}) as the severity class varied. However, unlike vegetation C, soil organic C decreased since the fire. The difference between the fire and the no-fire scenario increased to 2038.6-5827.1 g C m^{-2} in the 25th year after the fire. This is because the reduced vegetation provides less litter C to the soil so the soil organic C would reduce until vegetation fully recovers (Fig. 4d). Soil physical properties such as soil moisture and soil temperature also changed after the fire. In particular, soil moisture (in % of total porosity) increased after fire, more under more severe fires. However, this change was small enough (ranging between -0.07-0.08% in the first year after the fire while 0.005-0.17% in the 25th year after the fire) so that the soil moisture change had a trivial contribution to the dynamics of post-fire C budget (Fig. 4e). Soil temperature increased among all severity levels, with a range of 1.32-1.34 °C in the year after fire and 0.91-1.11 °C in the 25th year after the fire (Fig. 4f). In the first year after fire, R_H increased between 19.7-23.2 g C $yr^{-1} \cdot m^2$ for fires with the dNBR below 300, while decreased between 0.6-109.2 g C $yr^{-1} \cdot m^2$ for fires with the dNBR above 300. However, even though the R_H for low-severity fires increased in the first few years after the fire, it decreased with time in response to the lower soil organic C. In particular, in the 25th year after the fire, the R_H increased between -10.3- -13.0 g C $yr^{-1} \cdot m^2$ for fires with the dNBR below 300, and decreased between 20.9-73.1 g C $yr^{-1} \cdot m^2$ for fires with the dNBR above 300 (Fig. 4g).

NEP decreased after fire mainly due to less vegetation, ranging between 19.8-122.0 g C $yr^{-1} \cdot m^2$ with an average of 113.4 g C $yr^{-1} \cdot m^2$. The largest NEP decrease was found in low severity fires, i.e. dNBR < 100, where R_H increased most after the fire, while the smallest decrease was found in high severity fires, i.e. dNBR > 600, where R_H decreased the most. In the 25th year after the fire, with the increase of NPP and the decrease of R_H, NEP increased and the difference between the fire and no-fire scenario decreased to -19.8-8.8 g C $yr^{-1} \cdot m^2$ (Fig. 4h).

In addition, for all eight variables in Fig. 4 (vegetation C, net N mineralization, NPP, soil organic C, soil moisture, soil temperature, R_H and NEP), their averages (i.e. the black lines) are in close agreement with the two levels of burn severity of 100 <= dNBR <= 200 and 200 <= dNBR <= 300, since the majority of fires have severity within this range (Fig. 1b).

Impact of burn severity on fire emission patterns. Under different burn severity levels, the primary source of C emission was different. We further analyzed the proportion of vegetation and soil combustion during the fire, and the temporal pattern of post-fire emission (Supplemental Fig. 2a). When the burn severity was relatively low (dNBR < 300), the during-fire emission was dominated by vegetation combustion while the soil

was almost unburned. Under more severe fires, soil combustion dominates the emission, which was 30.4±14.8%, 56.1±9.2%, 65.9±6.8% and 72.0±5.1% when dNBR was between 300-400, 400-500, 500-600 and above 600, respectively.

Since soils barely combust when dNBR is below 300, the proportion of direct soil emission out of the total post-fire soil emission (i.e. direct soil emission plus accumulative R_H since fire) was close to 0 (Supplemental Fig. 2b). This value became larger with the increase in burn severity and the amount of soil combustion and declined after fire since the cumulative R_H accounted for a larger proportion. The contribution of direct soil emission out of soil total post-fire emission decreased from 78.0% to 13.9%, 92.1% to 25.6%, 93.1% to 49.9% and 97.9% to 67.7% when dNBR ranged between 300-400, 400-500, 500-600 and above 600, respectively. Notably, since severe fires tended to reduce post-fire R_H, as discussed earlier, the proportion of direct soil emission decreased slower for severe fires. In particular, the value dropped by 64.1% (dNBR: 300-400), 66.5% (dNBR: 400-500), 43.2% (dNBR: 500-600), and 30.2% (dNBR: > 600) respectively, in the 25 years since burned.

A different pattern of C emissions was found for relative low severity (dNBR < 300) fires and a similar pattern was found for relative higher severity (Supplemental Fig. 2c) fires. During-fire emissions accounted for a large portion of the total ecosystem emissions at the early stage after a low-severity fire (87.3%-89.0% at the year of fire), due to the combustion of vegetation. However, this proportion decreased quickly after the fire since R_H was hardly influenced and it made large contributions to the emission (37.4-39.6%). The pattern under severe burn was generally consistent between Supplemental Fig. 2b and c, as the emission from soil combustion becomes larger.

The difference between total emissions with and without considering fires and the during-fire emission is presented in this study as a ratio (Supplemental Fig. 2d). When the ratio is larger than one, a fire event results in a higher proportion of indirect emissions via R_H. However, when the ratio is close to one, the fire even triggers a destruction of the standing vegetation and reduces post-fire R_H. The lower severity corresponds with higher ratios in the early post-fire stage. With time, the ratio gradually drops to 0 as the ecosystem recovers back to the pre-fire stage, unless the forest stand is replaced by the other vegetation types. However, for all severity classes, the ratio increased in the 25 years after the fire, suggesting that the ecosystem and vegetation were yet to recover to the pre-fire stage. As a result, plant productivity did not exceed the ecosystem respiration.

Discussion

Combustion emissions. Our estimated C emissions during the fire were lower than in some previous studies in both Alaska [36-40] and Canada [16,41]. However, it falls within the range of some of previous studies [29,40,42](Supplemental Table 1).

During 1986-2016, the average regional combustion emissions were 7.2 Tg C yr^{-1} for Alaska, higher than the 50-year average [43] (Table 1). Compared with the previous estimation [36], our estimation for emissions during 2001-2012 is lower, which is expected since our emission rate per unit area is also lower (Supplemental Table 1). Meanwhile, our estimation for 2004 is slightly lower while for 2006-2008 it is higher [38]. For Canada, the average combustion emission was 49.9 Tg C yr^{-1}. Our estimation of annual average during 1990-1997 is higher than previously reported values [29], as a result of higher emission rate per unit area. Similarly, for North American boreal forests, our estimation

was 57.1 Tg C yr^{-1} for 1986-2016 and 44.9 for 1997-2009, which is lower than the previous study with the lower emission rate per unit area [44].

The possible reason for our estimation being lower than some field measurements is that field measurements tend to select samples from core areas in the fire perimeter while excluding unburned and low-severity patches. However, these patches are included in the fire perimeter used to extract the dNBR values and result in a lower mean severity in our study. According to an Alaska field study [37], the mean combustion emission within the fire perimeter (1.98 ± 0.34 kg C m^{-2}) was lower than the mean in the core burn area (2.67 ± 0.40 kg C m^{-2}) and at the field sites (2.88 ± 0.23 kg C m^{-2}).

Our estimation is also lower than other model estimates [36,38,39,41,44], possibly due to the underestimation of the combustion by the dNBR. As discussed earlier, although relatively high correlations between dNBR and CBI are found in many black spruce-dominated boreal forests [45-48], CBI performs low in estimating the proportion of canopy combustion ($R^2 = 0.15$, [42]). Furthermore, the correlation between dNBR and overstory CBI is relatively poor ($R^2 = 0.31$-0.37, [47]), while the correlation between overstory CBI and the proportion of vegetation combustion is better ($R^2 = 0.44$, [42]). This indicates that the dNBR has a significant uncertainty in estimating the proportion of canopy combustion. Overstory CBI is reported to saturate at high values and hardly increase as the dNBR value increases [47]. Therefore, the proportion of vegetation combustion could be underestimated for severe fires. In addition, the studies using dNBR to estimate combustion emission indicate that dNBR saturates when reaching approximately 1000 and hardly detects higher field burn severity [37]. This may also contribute to the lower combustion emission compared with those studies estimated by wood fuel types (e.g. black spruce, deciduous forest, and low shrub) [29,38]. However, the influence of the dNBR saturation should be limited since there are very rare fires with a mean dNBR value higher than 1000.

In addition, there are other uncertainties in using dNBR to estimate the fire emissions. First, environmental factors such as moisture conditions, temperature, slope, elevation and time of burn were not considered in our study. However, studies have suggested that these factors could influence the burn severity [38,39]. In particular, fire area and emission tend to peak in summer in response to the high vapor pressure deficit [49], and the fuels tend to be wetter and more difficult to burn at lower elevation sites [36]. Therefore, including environmental factors and time of burn may improve the correlation between the dNBR and ground combustion proportion. Second, in the simulation, the boreal forest is taken as an entire ecosystem type without classifying it into more detailed ecozones. Moreover, the relationship between the dNBR and combustion proportion has been established on black spruce-dominated forests. However, part of the NA boreal forests is dominated by white spruce, which performs differently in terms of dNBR-CBI relationships. In particular, the black spruce forest shows higher dNBR values than the white spruce forest under a given field burn severity index due to greater canopy combustion [37]. When using the dNBR-CBI relationship derived from black spruce forest to estimate the CBI of a white spruce forest fire, the CBI value and the burn emission would be underestimated.

Post-fire C dynamics. The differences in C balance between pre-fire and post-fire conditions are mainly in two aspects: net plant productivity (NPP) and soil respiration (R_H). In our simulation, NPP increases linearly after the fire, which is consistent with other studies [50]. The trend of post-fire NPP is in close agreement with the simulated net N mineralization rate (Fig. 4b & c). During the year of fire, net N mineralization rate decreases likely due to the massive reduction in soil N [34]. In agreement with this study, both previous TEM simulation [34] and field measurements [51] show the same trend of decrease in net N mineralization immediately after the fire and then a gradually increases to the pre-fire condition. With the recovery of net N mineralization, more N becomes available to plants, triggering a faster recovery. In addition to net N mineralization, the time NPP takes to recover is also influenced by burn severity (Fig. 4c). Even light fires require more than 25 years to recover. However, the dataset from Boreal Plains ecozone of Alberta showed NPP becomes stable in 20-30 years after fire [50]. The results from previous studies consistent with our results [52,53], hinting at NPP peaks when the stand age is 50-75 years. Furthermore, an even longer recovery time has been preciously suggested with NPP peaks in 80-100 years after the fire [34].

R_H is influenced by soil moisture, soil temperature, soil organic C content and microbial community [24]. Although microbial community shift under fire disturbance is not considered by the model, the change in soil temperature, soil moisture and soil organic C could partly explain the change in R_H. Our results show that soil moisture increases after the fire, with a higher increase in more severe fires. This is consistent with the previous findings [20], suggesting that such a behavior is attributed to a decline in vegetation water uptake and soil infiltration rates [54]. The soil temperature increases after the fire, in agreement with field observation [17,20], and the model simulation [34]. The magnitude of the change reported here (1-2 °C) is close to the values reported by previous modelling (e.g., 1.5-4.5 °C [34]). However, a previous field measurement suggests higher values (5-8 °C [17]), the reason of which could be that their measurement is in non-permafrost area, while our result is generated from both permafrost and non-permafrost areas. In addition to increasing soil temperature and moisture, fire also increases the temperature sensitivity of microbial respiration (i.e., Q_{10}, [55]). In our simulation, when the fire was relatively less severe, i.e. dNBR < 300, the soil microbial activities are more intensive under moister and warmer conditions. However, since the soil is hardly burned, the negative effect of soil organic C decline is minor and could not override positive effect of wetter and warmer soil condition on R_H. This agrees with previous report [17]. On the contrary, when dNBR is higher than 300, the negative effect of soil organic C decrease would offset the increased microbial activity, resulting in a lower R_H (Fig. 4g).

However, in this simulation, R_H decreased likely due to the lower microbial abundance [56] and the decreased soil organic C under moderate-to-high severity fires (Fig. 4g). This trend is consistent with field measurement [13] and model estimation [34]. Similarly, R_H decreases shortly after fire in a Canadian boreal forest site [57], and a study on the entire boreal area suggests that around three decades for R_H to stabilize after the fire [23]. On the contrary, when burn severity is low and the soil is not combusted, decline in R_H was not observed in our study. Regardless of the burn severity, the post-fire R_H tends to account for a certain proportion of the total fire-related emissions (Supplemental Fig. 2c & d).

This post-fire emission is reported to be almost three times as large as the during-fire emission in the Northern Hemisphere as reported in a previous modelling study [58].

In our simulation, NEP recovered almost to the pre-fire level in the 25th year after the fire, (Fig. 4h), while a previous modelling indicates forest does not become a C sink until 35-50 years after fire [34]. This difference might result from the different burn severities used in our simulations. In addition, whether a forest becomes a C sink or a source after the fire in a given period also differs by the species composition and climate of the site [3]. However, it should be noted that even if the NEP of a forest ecosystem is positive, it is not necessarily a 'true C sink' as long as the C emitted during combustion is not compensated by the post-fire productivity. In our simulation, even if the cumulative NEP is positive (59 Tg), the NA boreal ecosystem is still a net C source since net C assimilation did not exceed combustion emissions. As a result, the C storage in both soil and vegetation keeps decreasing (Supplementary Fig. 1b & c). This is supported by the finding that Canadian boreal ecosystems had become a C source in the 1980s, when other disturbance factors such as insects, clear-cur harvesting were considered [2]. Similarly, the northern high latitudes (above 50°N) are reported to be a current C source by 276 Tg C yr^{-1}, although more ecosystem types other than boreal forests are included [59].

It should be noted that our model still oversimplifies the fire impacts on the complex ecosystem processes. For example, the fires tend to leave dead wood legacy, cause delayed mortality and delayed decomposition, which are not considered in the model while they still influence the temporal pattern of post-fire R_H dynamics [60]. Furthermore, while the fire-induced active layer deepening and its impacts on C and N dynamics are modeled, the effects of thermokarst-induced land morphology and hydrological dynamics on C dynamics are not considered in this analysis [61]. In addition, satellite images show that some boreal forests are more dominated by deciduous species during post-fire succession [62], but this change in land cover is not considered in the present simulation. Therefore, better knowledge on the post-fire legacy composition and the landscape changes shall help improve the accuracy of our C estimates.

Methods

Overview. We extracted the dNBR value for 23,750 NA boreal fires during 1986-2016 via Google Earth Engine (GEE) to represent the burn severity. dNBR values were further correlated with Composite Burn Index (CBI), a field-measured burn severity index, which was used to estimate the proportion of vegetation and soil C consumption in the Terrestrial Ecosystem Model [34]. Model inputs include monthly air temperature, precipitation, vapor pressure and cloudiness, soil texture, plant functional type, elevation and annual CO_2 concentration (Mauna Loa). Three fire areas in Canadian boreal forest with observation data were used to evaluate the model. Regional simulations were conducted for Alaskan and Canadian boreal forests to quantify the C budget during 1986-2016.

Burn severity estimation. The fire history data for Alaska and Canada are available on Alaska Interagency Coordination Center and Natural Resources Canada, respectively. These records were spatially intersected with the boundary of North American boreal forest provided by Natural Resources Canada so that only boreal fires were kept. The fire year, fire perimeter and fire area were recorded, while the burn severity data was not available (Fig. 1).

Since the 1980s, the estimation of burn severity with satellite data became possible. Current fire-related satellite indices include difference Normalized Burn Ratio (dNBR) and relative differenced Normalized Burn Ratio (RdNBR). Both dNBR and RdNBR are calculated from Normalized Burn Ratio

(NBR), which are defined by the near infrared (Band 4) and short-wave infrared (Band 7) bands of Landsat TM/ETM data [63]:

$$NBR = \frac{(B4 - B7)}{(B4 + B7)} \times 1000 \quad (5)$$

$$dNBR = NBR_{prefire} - NBR_{postfire} \quad (6)$$

RdNBR is simply the relative form of dNBR and both of their values positively correlate with burn severity. In particular, a dNBR value below 100 tends to indicate no-fire, while the dNBR value for burned area usually ranges between 100 and 1300, with the average of 200-400 reported in Alaska boreal field sites [45,64]. Although RdNBR performs better than dNBR for burn severity classification, the correlations between RdNBR and dNBR with field burn severity indices show close coefficient efficiency [48]. We extracted the mean dNBR value for each fire event in the North American boreal forest area during 1986-2016 via Google Earth Engine (GEE). For each fire, its mean dNBR value was subtracted by a background dNBR to remove the background variation. The background value was initially defined as the mean dNBR value in a buffer zone at the year of fire, while the buffer zone was the area between 1500m and 1800m out of the fire boundary. In case of creating a buffer-zone takes up a large GEE's computation capacity, the dNBR value during one year before fire within the fire perimeter was used as background value instead. Although these two methods show some deviations at the low-value end, they generally fall on the 1:1 line (Supplemental Fig. 3a). Among the total of 23,750 (Alaska: 2346 versus Canada: 21404), 126 (Alaska: 51 versus Canada: 75) fire events do not have available images due to the limitation of satellite coverage. Their dNBR values were estimated from the average of ten fires closest in size (Fig. 2b showing the gap-filled dNBR of all North American boreal fires in 1986-2016).

Although there is no study to directly relate dNBR to the proportion of C removal during a fire, it is possible to build up their indirect correlation. Many studies have proposed or reviewed the correlations between dNBR and a field-based burn severity index, the Composite Burn Index (CBI), in boreal forests [45,46,48]. When measuring CBI, forests are divided into five layers vertically, and a CBI score is given to each layer according to the post-fire condition. Then these five scores are combined into a total CBI along a 0-3 scale, with higher values representing more severe burning [64]. The correlation between CBI and dNBR in our study was based on published field data [48,65] in Canadian boreal forests (Supplemental Fig. 3b). The linear regression equation is:

$$CBI = 0.0023 \times dNBR + 0.5561 \ \ (R^2 = 0.57) \quad (7)$$

Therefore, for each fire event, the CBI value was estimated from its dNBR value. Based on the field measurements of 38 black spruce (*Picea mariana*) dominated boreal forest sites, a previous study has established a linear relationship between CBI and the proportion of C removal in vegetation and soil [42]:

$$organic\ soil\ C\ combustion\ (\%) = 51.42 \times CBI - 63.49 \ \ (R^2 = 0.50) \quad (8)$$

$$canopy\ C\ combustion\ (\%) = 14.15 \times CBI + 48.63 \ \ (R^2 = 0.15) \quad (9)$$

These equations were used to estimate soil and vegetation C removal based on CBI values. Notably, the correlation between CBI and the proportion of vegetation C combustion is relatively low, which also introduces uncertainties to C emission modelling. However, this influence should be acceptable since the majority of C is stored in soils rather than vegetation.

Model and Data. TEM is a process-based biogeochemical model that can simulate C and nitrogen (N) dynamics at regional scales. The model has been used previously to simulate fire impacts on C dynamics of black spruce-dominated boreal forests in Alaska [34]. In this version, TEM is integrated with a hydrology module and a soil thermal module. After fire disturbance, foliage is assumed to be linearly recovering for the first 5 years, and then tends to show a sigmoid trend. Moss layer thickness recovery is described by an exponential function of the year after the fire. Simulated net N mineralization dynamics shows close agreement with the trend of vegetation C. The model captures field measurements well at a fire chronosequence in Alaska. A more detailed description of the model structure and parameters can be found in ref [34]. Here we use the model to simulate the fire impacts on C dynamics of North America boreal forests. The model was first upgraded from a serial version into a parallel version to efficiently conduct

large-scale simulations. After that, dNBR was incorporated into model simulations to account for the impacts of burn severity.

Monthly air temperature (°C), vapor pressure (hPa), precipitation (mm) and cloud cover (percentage) data were used to drive the model. The climate record (1901-2016) derived from observations and resampled into 0.5°×0.5° grid was provided by the Climate Research Unit of the University of East Anglia (version 4.03) [66]. In addition, spatially-explicit data of soil texture (percentage of silt, clay and sand, [67]), elevation [34] and plant functional type [68] were also used. Atmospheric CO_2 data were obtained from Mauna Loa annual CO_2 records provided by Global Monitoring Laboratory, Earth System Research Laboratories. Fire data including fire year and burn severity are discussed in Section burn severity estimation.

Model verification. The model was calibrated using the field data from black spruce forest ecosystems in interior Alaska, where the model agreed with field observations in terms of post-fire 10cm soil temperature, 20cm soil temperature, soil heterotrophic respiration (R_H) and soil organic C [34]. Here we applied the satellite-derived burn severity indices to re-evaluate the accuracy of the model with the field data collected in three Canadian boreal sites burned in 1969, 1990 and 2012, respectively, dominated by black spruce and white spruce (*Picea glauca*). For these sites, vegetation C, soil organic C, soil N, 5cm soil temperature and 10cm soil temperature were measured in August 2015 [55,57].

Before carrying out simulation for these sites, their burn severity should be defined. Although extracting the dNBR for the fires in 1990 and 2012 was feasible, there was no satellite record for the fire in 1969. However, the proportion of soil combustion can be coarsely estimated from soil organic matter depth, which was observed for these sites [42]. For the fire in 1990 and 2012, the approximate soil combustion proportions were 40% (10.2cm organic layer remaining) and 65% (5.0cm organic layer remaining), respectively. The dNBR values calculated from the correlation between the proportion of soil C removal were 633.28 and 844.67, respectively. The actual dNBR values for 1990 and 2012 sites were then extracted from GEE for comparison. The calculated and actual dNBR values were close (633.28 versus 686.72, and 844.67 versus 811.49, Supplemental Table 2). Therefore, for the site burned in 1969, it is reasonable to estimate the input dNBR value from the depth of the soil organic layer, with 506.5 corresponding to an organic layer depth of 14.1cm.

In terms of C stocks, the model estimated vegetation C and soil organic C tend to fall within the range of field measurement, except for the vegetation C in the site burned in 1990 (measurement: 698.9 ± 178.2 versus estimated: 889.3) (Supplemental Table 2). However, since the model estimation is only 12.2 g C m^{-2} higher than the upper bound of the field measurement, we assume the model is still reliable in estimating field C stocks. For soil temperature, the 5cm soil temperature at the site burned in 1990 and the 10cm temperature at the site burned in 1969 showed discrepancies between model estimation and field measurement. However, these discrepancies are not large. In particular, for the former, the estimation is 1.3°C lower than the lower bound of measurement; while for the latter, the estimation is 0.9°C higher than the upper bound of measurement. The soil organic N, model estimation tends to be higher or lower than the observation. However, the discrepancy between modeled and measure soil organic N is not large, which will not affect the estimation of C dynamics under the fire disturbance (Supplemental Table 2).

Regional carbon dynamics simulations. Two regional simulations were conducted with and without considering the impacts of fire disturbance. In the no-fire simulation, the North American boreal forest was gridded into 0.5°×0.5° cells and the proportion of forest area within each cell was calculated. After spinning up for 120 years, a transient simulation was conducted for each cell during 1986-2016. When considering fire impacts, the fire polygons were dissected into units with unique fire history. Each unit was intersected with the 0.5°×0.5° grid to create 'cohorts' with unique cell coordinate and fire history [26]. Then the area proportion of each cohort out of the boreal forest in the same cell was calculated. We run the simulation for each cohort, and the output values of each cohort and the no-burn areas were weighted by their area to get the mean of the cell.

When analyzing the C stock and flux of the entire North American (NA) boreal forest region, for each cell, the mean value of soil organic C, vegetation C, net ecosystem productivity (NEP), net primary productivity (NPP) and R_H were multiplied by the area of boreal forest in that cell to get the cell total value. The aggregation of all cells is the total value for the NA boreal forests. During 1986-2016, at the regional scale, the C balance (CB) under no fire disturbance is:

$$CB = \sum_{1986}^{2016} NEP \quad (10)$$

By considering fire impacts, the regional carbon sink and source activities (C balance (fire), CBF) are:

$$CBF = \sum_{1986}^{2016} NEP - \sum_{1986}^{2016} burn \quad (11)$$

Where SoilC is soil organic C storage, and VegC is vegetation C storage. NEP is the annual NEP and burn is the annual C vegetation and soil combustion. NEP is the difference between NPP and R_H.

Acknowledgments

This study is financially supported by a NSF project (#1802832), a United States Geological Survey project (#G17AC00276) and Department of Energy projects (#DE-SC0008092 and #DE-SC0007007), as well as the Academy of Finland projects 286685, 294600, 307222, 291691, 326818 and 323997.

Data access

All data used in this manuscript can be accessed in Purdue University Research Repository (https://purr.purdue.edu/publications/3532/1).

Author contributions

Bailu Zhao: Conducted modeling analysis and wrote the manuscript
Qianlai Zhuang: Conceive the study and wrote the manuscript
Narasinha Shurpali: Coordinated the modeling and field data teams and reviewed the manuscript
Kajar Köster: Collected field data at Canadian boreal forest sites and reviewed the manuscript
Frank Berninger: Collected field data at Canadian boreal forest sites and reviewed the manuscript
Jukka Pumpanen: Collected field data at Canadian boreal forest sites and reviewed the manuscript

Competing interests

There is no Competing interests among the authors.

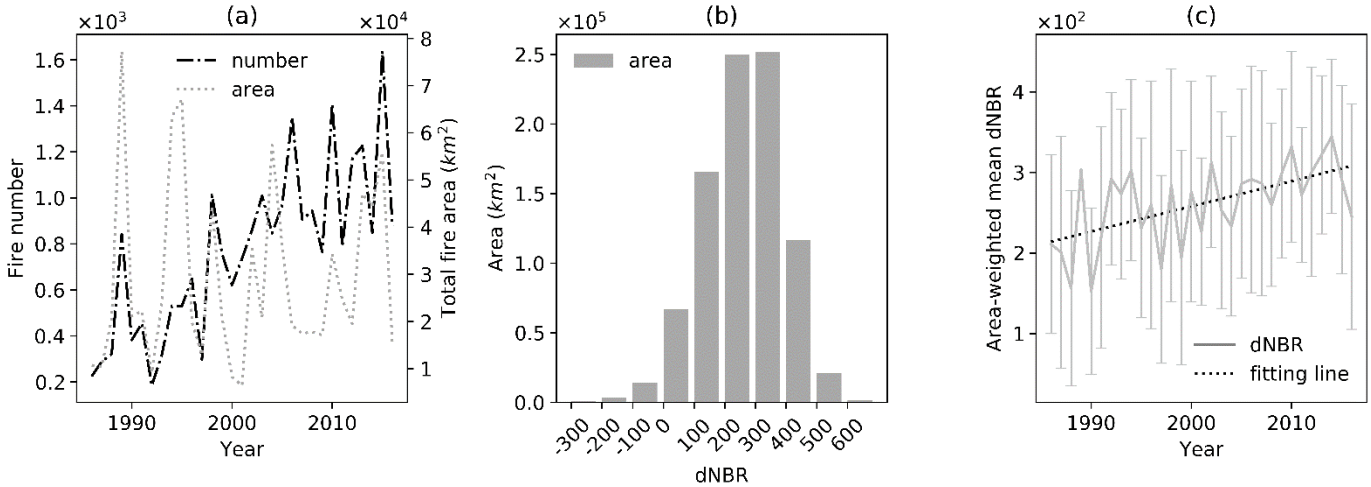

Fig. 1. Summary of the fire regime during 1986-2016: (a) Variations of the fire area and fire number in the North American boreal forests; (b) Histograms of dNBR (difference Normalized Burn Ratio), i.e. burn severity, in the North America boreal forests. The heights of grey bars are the total area of fires in which average dNBR is within the threshold indicated by the x axis. (c) Annual dNBR variation and trend of the fires in North American boreal forests.

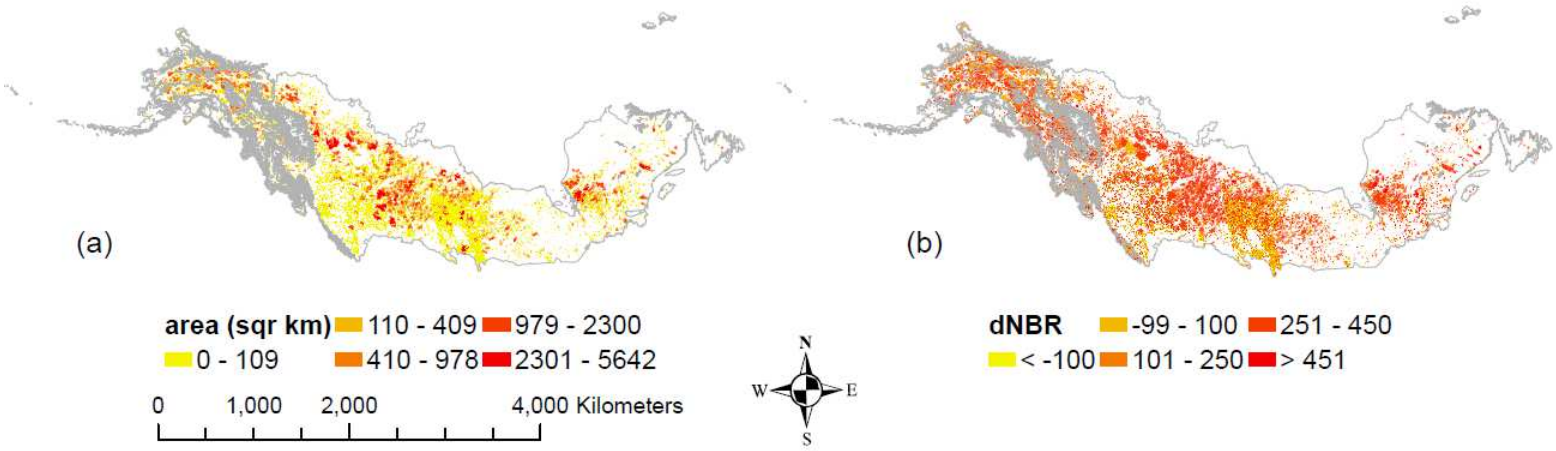

Fig. 2. Fire area and burn severity (as dNBR) during 1986-2016 in North America boreal forest. (a) fire area in km^2. (b) burn severity measured by the mean dNBR value within its perimeter. For both panels, the grey lines show the boundary of boreal forest.

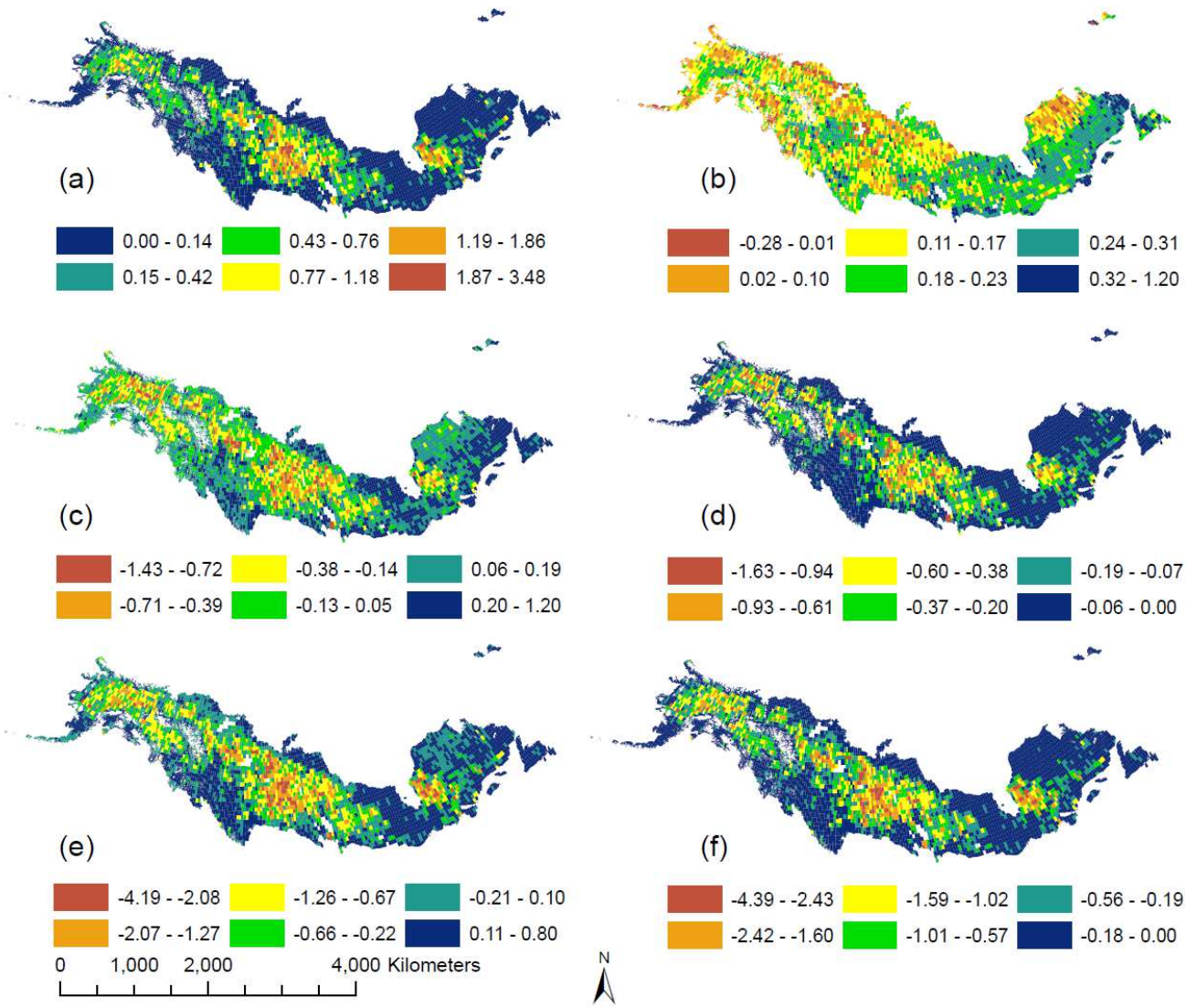

Fig. 3. Spatial pattern of C sequestration and emission, accumulated for 1986-2016 (Gg km^{-2}): (a) Total emissions from direct combustion (both vegetation and soil); (b) Cumulative NEP without considering fires, i.e. the change in ecosystem C storage when there is no fire; (c) Cumulative NEP considering fires; (d) Difference of cumulative NEP with and without considering fires (the former minus the latter); (e) Changes in ecosystem C storage considering fires; (f) Difference of ecosystem C storage between simulations with and without fires (the former minus the latter).

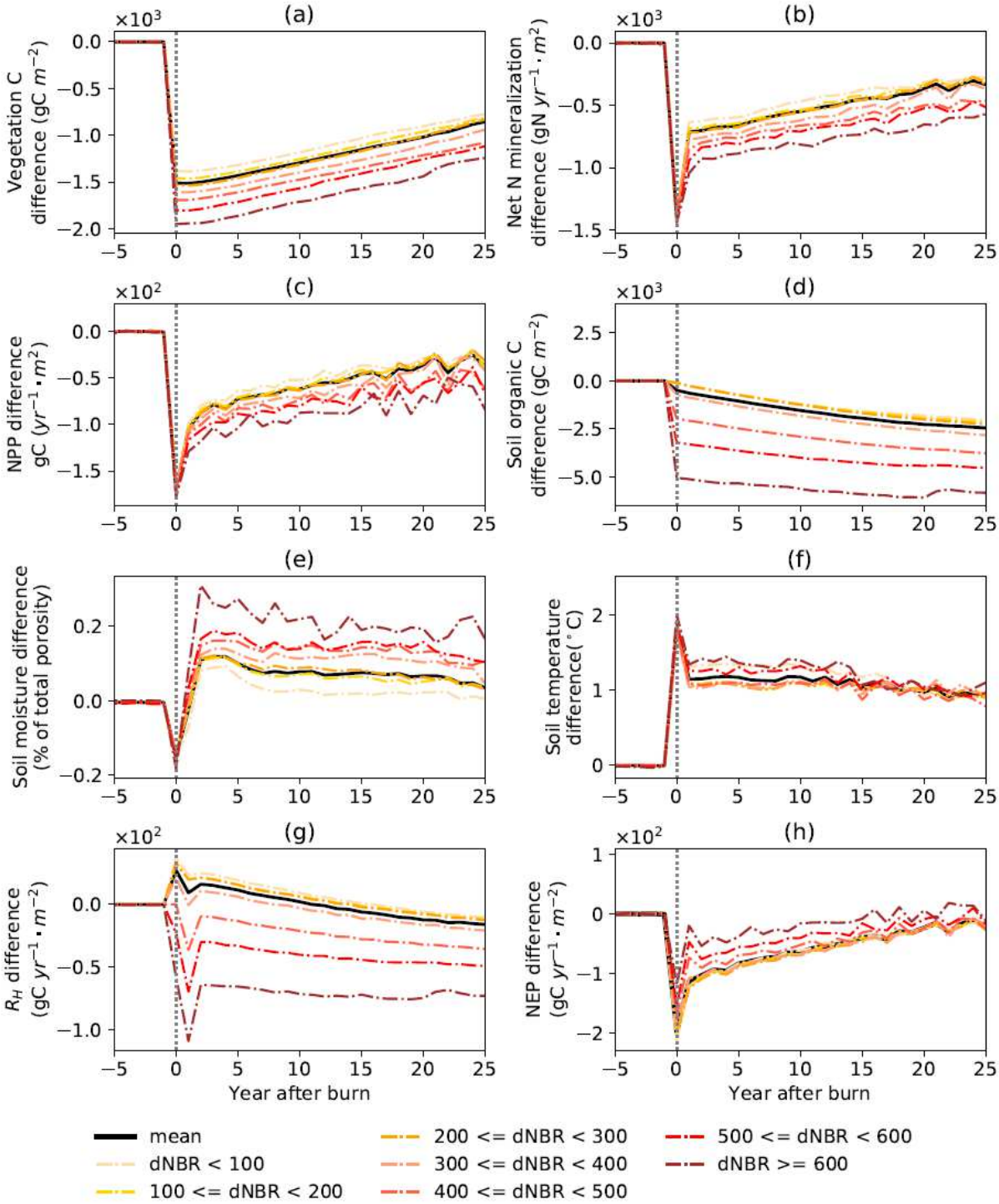

Fig. 4. Difference of carbon pools and fluxes between the fire and the no-fire scenarios (the no-fire minus the fire scenario) under different levels of burn severity. Only cohorts burned once (95.2% of the total burned area) are used for calculation. The values of each curve is the average of all cohorts with corresponding dNBR values: (a) Vegetation C (gC m^{-2}); (b) annual net N mineralization (gN $yr^{-1} \cdot m^{-2}$); (c) annual NPP (gC $yr^{-1} \cdot m^{-2}$); (d) soil organic C (gC m^{-2}); (e) soil moisture (% of total porosity); (f) soil temperature (°C); (g) Rh (gC $yr^{-1} \cdot m^{-2}$); (h) NEP (gC $yr^{-1} \cdot m^{-2}$).

Table 1. Comparison on regional combustion emission per year

Region	Time	Combustion (Tg C yr^{-1})	Source
Alaska	**1986-2016**	**7.2**	**This study**
	1950-2000	5.8	French, et al. [43]
	2001-2012	15	Veraverbeke, et al. [36]
		10.0	**This study**
	2004	42.4	Kasischke and Hoy [38]
		40.5	**This study**
	2006-2008	0.6	Kasischke and Hoy [38]
		1.2	**This study**
Canada	**1986-2016**	**49.9**	**This study**
	1959-1999	27 ± 6	Amiro, et al. [29]
	1990-1999	39	Amiro, et al. [29]
		52.7	**This study**
North America	**1986-2016**	**57.1**	**This study**
	1997-2009	54	van der Werf, et al. [44]
		44.9	**This study**

References

1 Kasischke, E. S. & Stocks, B. J. *Fire, Climate Change, and Carbon Cycling in the Boreal Forest*. (Springer-Verlag New York, 2000).

2 Kurz, W. A. & Apps, M. J. A 70-YEAR RETROSPECTIVE ANALYSIS OF CARBON FLUXES IN THE CANADIAN FOREST SECTOR. *Ecological Applications* **9**, 526-547, doi:10.1890/1051-0761(1999)009[0526:AYRAOC]2.0.CO;2 (1999).

3 Amiro, B. D. *et al.* Carbon, energy and water fluxes at mature and disturbed forest sites, Saskatchewan, Canada. *Agricultural and Forest Meteorology* **136**, 237-251, doi:https://doi.org/10.1016/j.agrformet.2004.11.012 (2006).

4 Li, F., Lawrence, D. M. & Bond-Lamberty, B. Impact of fire on global land surface air temperature and energy budget for the 20th century due to changes within ecosystems. *Environmental Research Letters* **12**, 044014, doi:10.1088/1748-9326/aa6685 (2017).

5 Gillett, N. P., Weaver, A. J., Zwiers, F. W. & Flannigan, M. D. Detecting the effect of climate change on Canadian forest fires. *Geophysical Research Letters* **31**, doi:10.1029/2004GL020876 (2004).

6 Kasischke, E. S. & Turetsky, M. R. Recent changes in the fire regime across the North American boreal region—Spatial and temporal patterns of burning across Canada and Alaska. *Geophysical Research Letters* **33**, doi:10.1029/2006GL025677 (2006).

7 de Groot, W. J., Flannigan, M. D. & Cantin, A. S. Climate change impacts on future boreal fire regimes. *Forest Ecology and Management* **294**, 35-44, doi:https://doi.org/10.1016/j.foreco.2012.09.027 (2013).

8 Rogers, B. M., Soja, A. J., Goulden, M. L. & Randerson, J. T. Influence of tree species on continental differences in boreal fires and climate feedbacks. *Nature Geoscience* **8**, 228, doi:10.1038/ngeo2352 https://www.nature.com/articles/ngeo2352#supplementary-information (2015).

9 Montes-Helu, M. C. *et al.* Persistent effects of fire-induced vegetation change on energy partitioning and evapotranspiration in ponderosa pine forests. *Agricultural and Forest Meteorology* **149**, 491-500, doi:https://doi.org/10.1016/j.agrformet.2008.09.011 (2009).

10 Denslow, J. S. Patterns of plant species diversity during succession under different disturbance regimes. *Oecologia* **46**, 18-21, doi:10.1007/bf00346960 (1980).

11 Bond-Lamberty, B., Peckham, S. D., Ahl, D. E. & Gower, S. T. Fire as the dominant driver of central Canadian boreal forest carbon balance. *Nature* **450**, 89, doi:10.1038/nature06272 https://www.nature.com/articles/nature06272#supplementary-information (2007).

12 Gewehr, S., Drobyshev, I., Berninger, F. & Bergeron, Y. Soil characteristics mediate the distribution and response of boreal trees to climatic variability. *Canadian Journal of Forest Research* **44**, 487-498, doi:10.1139/cjfr-2013-0481 (2014).

13 Sullivan, B. W. *et al.* Wildfire reduces carbon dioxide efflux and increases methane uptake in ponderosa pine forest soils of the southwestern USA. *Biogeochemistry* **104**, 251-265, doi:10.1007/s10533-010-9499-1 (2011).

14 Post, W. M., Emanuel, W. R., Zinke, P. J. & Stangenberger, A. G. Soil carbon pools and world life zones. *Nature* **298**, 156-159, doi:10.1038/298156a0 (1982).

15 Tarnocai, C. *et al.* Soil organic carbon pools in the northern circumpolar permafrost region. *Global Biogeochemical Cycles* **23**, doi:10.1029/2008gb003327 (2009).

16 Walker, X. J. *et al.* Cross-scale controls on carbon emissions from boreal forest megafires. *Global Change Biology* **24**, 4251-4265, doi:10.1111/gcb.14287 (2018).

17 Kulmala, L. *et al.* Changes in biogeochemistry and carbon fluxes in a boreal forest after the clear-cutting and partial burning of slash. *Agricultural and Forest Meteorology* **188**, 33-44, doi:https://doi.org/10.1016/j.agrformet.2013.12.003 (2014).

18 Yoshikawa, K., Bolton, W. R., Romanovsky, V. E., Fukuda, M. & Hinzman, L. D. Impacts of wildfire on the permafrost in the boreal forests of Interior Alaska. *Journal of Geophysical Research: Atmospheres* **107**, FFR 4-1-FFR 4-14, doi:10.1029/2001jd000438 (2002).

19 Tsuyuzaki, S., Kushida, K. & Kodama, Y. Recovery of surface albedo and plant cover after wildfire in a Picea mariana forest in interior Alaska. *Climatic Change* **93**, 517, doi:10.1007/s10584-008-9505-y (2008).
20 Hamman, S. T., Burke, I. C. & Stromberger, M. E. Relationships between microbial community structure and soil environmental conditions in a recently burned system. *Soil Biology and Biochemistry* **39**, 1703-1711, doi:https://doi.org/10.1016/j.soilbio.2007.01.018 (2007).
21 Atchley, A. L., Kinoshita, A. M., Lopez, S. R., Trader, L. & Middleton, R. Simulating Surface and Subsurface Water Balance Changes Due to Burn Severity. *Vadose Zone Journal* **17**, doi:10.2136/vzj2018.05.0099 (2018).
22 Taş, N. *et al.* Impact of fire on active layer and permafrost microbial communities and metagenomes in an upland Alaskan boreal forest. *ISME J* **8**, 1904-1919, doi:10.1038/ismej.2014.36 (2014).
23 Ribeiro-Kumara, C., Köster, E., Aaltonen, H. & Köster, K. How do forest fires affect soil greenhouse gas emissions in upland boreal forests? A review. *Environmental Research* **184**, 109328, doi:https://doi.org/10.1016/j.envres.2020.109328 (2020).
24 Köster, K., Berninger, F., Lindén, A., Köster, E. & Pumpanen, J. Recovery in fungal biomass is related to decrease in soil organic matter turnover time in a boreal fire chronosequence. *Geoderma* **235-236**, 74-82, doi:https://doi.org/10.1016/j.geoderma.2014.07.001 (2014).
25 Conard, S. G. & A. Ivanova, G. Wildfire in Russian Boreal Forests—Potential Impacts of Fire Regime Characteristics on Emissions and Global Carbon Balance Estimates. *Environmental Pollution* **98**, 305-313, doi:https://doi.org/10.1016/S0269-7491(97)00140-1 (1997).
26 Balshi, M. S. *et al.* The role of historical fire disturbance in the carbon dynamics of the pan-boreal region: A process-based analysis. *Journal of Geophysical Research: Biogeosciences* **112**, doi:10.1029/2006JG000380 (2007).
27 French, N. H. F., Kasischke, E. S. & Williams, D. G. Variability in the emission of carbon-based trace gases from wildfire in the Alaskan boreal forest. *Journal of Geophysical Research: Atmospheres* **107**, FFR 7-1-FFR 7-11, doi:10.1029/2001JD000480 (2002).
28 Kajii, Y. *et al.* Boreal forest fires in Siberia in 1998: Estimation of area burned and emissions of pollutants by advanced very high resolution radiometer satellite data. *Journal of Geophysical Research: Atmospheres* **107**, ACH 4-1-ACH 4-8, doi:10.1029/2001JD001078 (2002).
29 Amiro, B. D. *et al.* Direct carbon emissions from Canadian forest fires, 1959-1999. *Canadian Journal of Forest Research* **31**, 512-525, doi:10.1139/x00-197 (2001).
30 Kasischke, E. S. *et al.* Influences of boreal fire emissions on Northern Hemisphere atmospheric carbon and carbon monoxide. *Global Biogeochemical Cycles* **19**, doi:10.1029/2004GB002300 (2005).
31 Seiler, W. & Crutzen, P. J. Estimates of gross and net fluxes of carbon between the biosphere and the atmosphere from biomass burning. *Climatic Change* **2**, 207-247, doi:10.1007/BF00137988 (1980).
32 Mouillot, F., Narasimha, A., Balkanski, Y., Lamarque, J.-F. & Field, C. B. Global carbon emissions from biomass burning in the 20th century. *Geophysical Research Letters* **33**, doi:10.1029/2005GL024707 (2006).
33 Cansler, C. A. & McKenzie, D. Climate, fire size, and biophysical setting control fire severity and spatial pattern in the northern Cascade Range, USA. *Ecological Applications* **24**, 1037-1056 (2014).
34 Zhuang, Q. *et al.* Modeling soil thermal and carbon dynamics of a fire chronosequence in interior Alaska. *Journal of Geophysical Research: Atmospheres* **107**, FFR 3-1-FFR 3-26, doi:10.1029/2001jd001244 (2002).
35 Zackrisson, O. Influence of Forest Fires on the North Swedish Boreal Forest. *Oikos* **29**, 22-32, doi:10.2307/3543289 (1977).
36 Veraverbeke, S., Rogers, B. M. & Randerson, J. T. Daily burned area and carbon emissions from boreal fires in Alaska. *Biogeosciences* **12**, 3579-3601, doi:10.5194/bg-12-3579-2015 (2015).
37 Rogers, B. M. *et al.* Quantifying fire-wide carbon emissions in interior Alaska using field measurements and Landsat imagery. *Journal of Geophysical Research: Biogeosciences* **119**, 1608-1629, doi:10.1002/2014jg002657 (2014).

38 Kasischke, E. S. & Hoy, E. E. Controls on carbon consumption during Alaskan wildland fires. *Global Change Biology* **18**, 685-699, doi:10.1111/j.1365-2486.2011.02573.x (2012).
39 Tan, Z., Tieszen, L. L., Zhu, Z., Liu, S. & Howard, S. M. An estimate of carbon emissions from 2004 wildfires across Alaskan Yukon River Basin. *Carbon Balance and Management* **2**, 12, doi:10.1186/1750-0680-2-12 (2007).
40 Randerson, J. T. *et al.* The Impact of Boreal Forest Fire on Climate Warming. *Science* **314**, 1130, doi:10.1126/science.1132075 (2006).
41 de Groot, W. *et al.* Estimating direct carbon emissions from Canadian wildland fires. *International Journal of Wildland Fire* **16**, doi:10.1071/WF06150 (2007).
42 Boby, L. A., Schuur, E. A. G., Mack, M. C., Verbyla, D. & Johnstone, J. F. Quantifying fire severity, carbon, and nitrogen emissions in Alaska's boreal forest. *Ecological Applications* **20**, 1633-1647, doi:10.1890/08-2295.1 (2010).
43 French, N. H. F., Goovaerts, P. & Kasischke, E. S. Uncertainty in estimating carbon emissions from boreal forest fires. *Journal of Geophysical Research: Atmospheres* **109**, doi:10.1029/2003JD003635 (2004).
44 van der Werf, G. R. *et al.* Global fire emissions and the contribution of deforestation, savanna, forest, agricultural, and peat fires (1997–2009). *Atmos. Chem. Phys.* **10**, 11707-11735, doi:10.5194/acp-10-11707-2010 (2010).
45 Allen, J. L. & Sorbel, B. Assessing the differenced Normalized Burn Ratio's ability to map burn severity in the boreal forest and tundra ecosystems of Alaska's national parks. *International Journal of Wildland Fire - INT J WILDLAND FIRE* **17**, doi:10.1071/WF08034 (2008).
46 French, N. H. F. *et al.* Using Landsat data to assess fire and burn severity in the North American boreal forest region: an overview and summary of results. *International Journal of Wildland Fire* **17**, 443-462, doi:https://doi.org/10.1071/WF08007 (2008).
47 Hoy, E., French, N., Turetsky, M., Trigg, S. & Kasischke, E. Evaluating the potential of Landsat TM/ETM+ imagery for assessing fire severity in Alaskan black spruce forests. *International Journal of Wildland Fire* **17**, 500-514, doi:10.1071/WF08107 (2008).
48 Soverel, N. O., Perrakis, D. D. B. & Coops, N. C. Estimating burn severity from Landsat dNBR and RdNBR indices across western Canada. *Remote Sensing of Environment* **114**, 1896-1909, doi:https://doi.org/10.1016/j.rse.2010.03.013 (2010).
49 Sedano, F. & Randerson, J. T. Multi-scale influence of vapor pressure deficit on fire ignition and spread in boreal forest ecosystems. *Biogeosciences* **11**, 3739-3755, doi:10.5194/bg-11-3739-2014 (2014).
50 Amiro, B. D., Chen, J. M. & Liu, J. Net primary productivity following forest fire for Canadian ecoregions. *Canadian Journal of Forest Research* **30**, 939-947, doi:10.1139/x00-025 (2000).
51 Turner, M. G., Smithwick, E. A. H., Metzger, K. L., Tinker, D. B. & Romme, W. H. Inorganic nitrogen availability after severe stand-replacing fire in the Greater Yellowstone ecosystem. *Proceedings of the National Academy of Sciences* **104**, 4782, doi:10.1073/pnas.0700180104 (2007).
52 Gower, S. T., McMurtrie, R. E. & Murty, D. Aboveground net primary production decline with stand age: potential causes. *Trends in Ecology & Evolution* **11**, 378-382, doi:https://doi.org/10.1016/0169-5347(96)10042-2 (1996).
53 Pare, D. & Bergeron, Y. Above-Ground Biomass Accumulation along a 230-Year Chronosequence in the Southern Portion of the Canadian Boreal Forest. *Journal of Ecology* **83**, 1001-1007, doi:10.2307/2261181 (1995).
54 Ice, G., Neary, D. & Adams, P. Effects of Wildfire on Soils and Watershed Processes. *Journal of Forestry* **102**, 16-20 (2004).
55 Aaltonen, H. *et al.* Temperature sensitivity of soil organic matter decomposition after forest fire in Canadian permafrost region. *Journal of Environmental Management* **241**, 637-644, doi:https://doi.org/10.1016/j.jenvman.2019.02.130 (2019).
56 Dooley, S. R. & Treseder, K. K. The effect of fire on microbial biomass: a meta-analysis of field studies. *Biogeochemistry* **109**, 49-61, doi:10.1007/s10533-011-9633-8 (2012).
57 Köster, E. *et al.* Carbon dioxide, methane and nitrous oxide fluxes from a fire chronosequence in subarctic boreal forests of Canada. *Science of The Total Environment* **601-602**, 895-905, doi:https://doi.org/10.1016/j.scitotenv.2017.05.246 (2017).

58 Auclair, A. N. D. & Carter, T. B. Forest wildfires as a recent source of CO2 at northern latitudes. *Canadian Journal of Forest Research* **23**, 1528-1536, doi:10.1139/x93-193 (1993).
59 Zhuang, Q. *et al.* CO2 and CH4 exchanges between land ecosystems and the atmosphere in northern high latitudes over the 21st century. *Geophysical Research Letters* **33**, doi:10.1029/2006GL026972 (2006).
60 Walker, X. J. *et al.* Increasing wildfires threaten historic carbon sink of boreal forest soils. *Nature* **572**, 520-523, doi:10.1038/s41586-019-1474-y (2019).
61 Osterkamp, T. E. *et al.* Observations of Thermokarst and Its Impact on Boreal Forests in Alaska, U.S.A. *Arctic, Antarctic, and Alpine Research* **32**, 303-315, doi:10.1080/15230430.2000.12003368 (2000).
62 Beck, P. S. A. *et al.* The impacts and implications of an intensifying fire regime on Alaskan boreal forest composition and albedo. *Global Change Biology* **17**, 2853-2866, doi:10.1111/j.1365-2486.2011.02412.x (2011).
63 Miller, J. D. & Thode, A. E. Quantifying burn severity in a heterogeneous landscape with a relative version of the delta Normalized Burn Ratio (dNBR). *Remote Sensing of Environment* **109**, 66-80, doi:https://doi.org/10.1016/j.rse.2006.12.006 (2007).
64 Key, C. & Benson, N. LA 1-51 (2005).
65 Epting, J., Verbyla, D. & Sorbel, B. Evaluation of remotely sensed indices for assessing burn severity in interior Alaska using Landsat TM and ETM+. *Remote Sensing of Environment* **96**, 328-339, doi:https://doi.org/10.1016/j.rse.2005.03.002 (2005).
66 Mitchell, T., Carter, T., Jones, P. & Hulme, M. A Comprehensive Set of High-Resolution Grids of Monthly Climate for Europe and the Globe: The Observed Record (1901–2000) and 16 Scenarios (2001–2100). *Tyndall Centre Working Paper* **55** (2004).
67 FAO-Unesco. *Soil map of the world*. Vol. 1 (Food and Agriculture Organization of the United Nations and the United Nations Educational, Scientific and Cultural Organization, 1974).
68 Melillo, J. M. *et al.* Global climate change and terrestrial net primary production. *Nature* **363**, 234-240, doi:10.1038/363234a0 (1993).

Figures

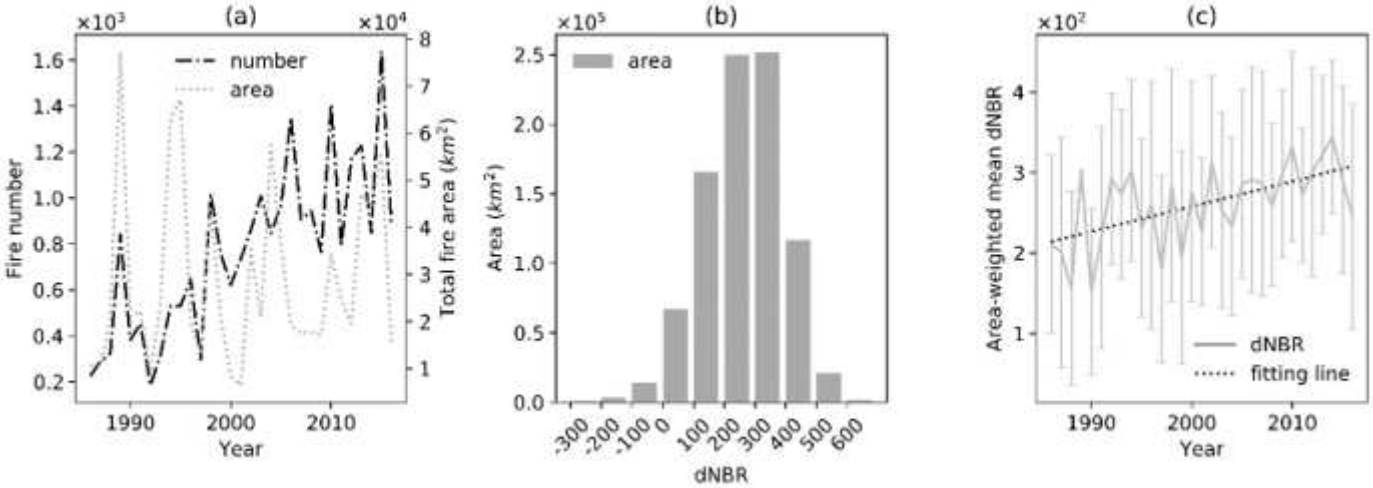

Figure 1

Summary of the fire regime during 1986-2016: (a) Variations of the fire area and fire number in the North American boreal forests; (b) Histograms of dNBR (difference Normalized Burn Ratio), i.e. burn severity, in the North America boreal forests. The heights of grey bars are the total area of fires in which average dNBR is within the threshold indicated by the x axis. (c) Annual dNBR variation and trend of the fires in North American boreal forests.

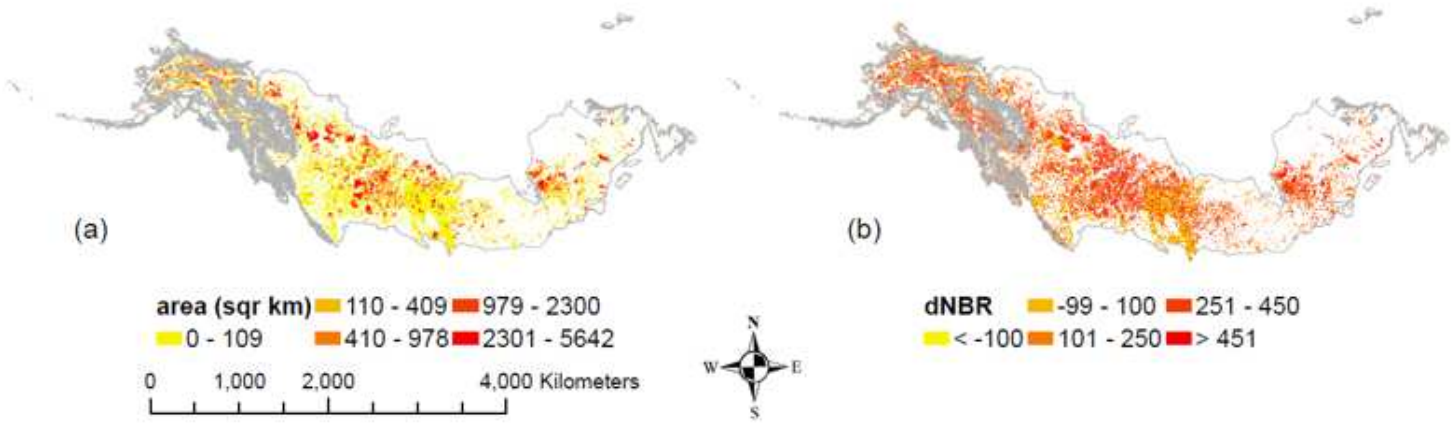

Figure 2

Fire area and burn severity (as dNBR) during 1986-2016 in North America boreal forest. (a) fire area in km2. (b) burn severity measured by the mean dNBR value within its perimeter. For both panels, the grey lines show the boundary of boreal forest.

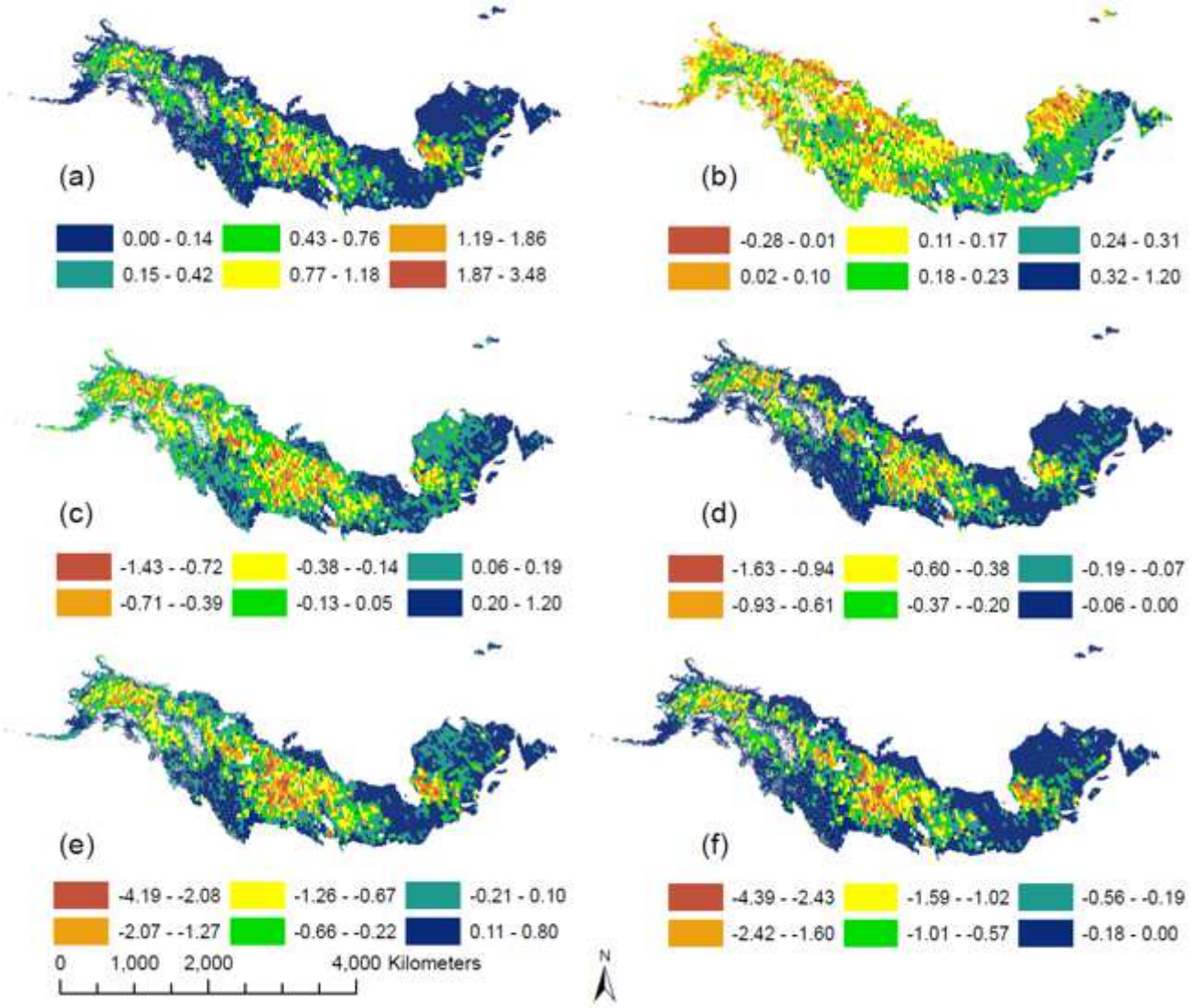

Figure 3

Spatial pattern of C sequestration and emission, accumulated for 1986-2016 (Gg km-2): (a) Total emissions from direct combustion (both vegetation and soil); (b) Cumulative NEP without considering fires, i.e. the change in ecosystem C storage when there is no fire; (c) Cumulative NEP considering fires; (d) Difference of cumulative NEP with and without considering fires (the former minus the latter); (e) Changes in ecosystem C storage considering fires; (f) Difference of ecosystem C storage between simulations with and without fires (the former minus the latter).

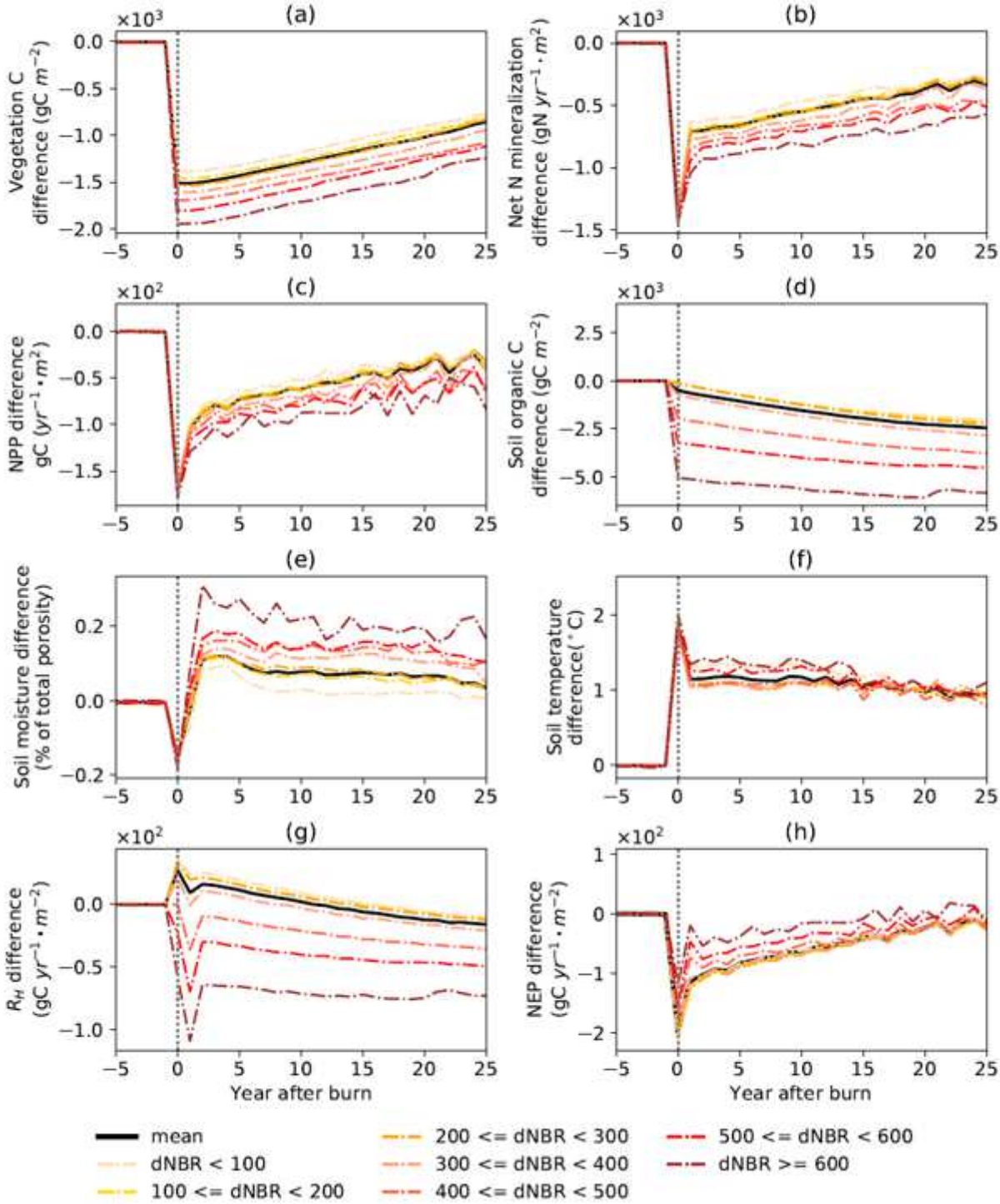

Figure 4

Difference of carbon pools and fluxes between the fire and the no-fire scenarios (the no-fire minus the fire scenario) under different levels of burn severity. Only cohorts burned once (95.2% of the total burned area) are used for calculation. The values of each curve is the average of all cohorts with corresponding dNBR values: (a) Vegetation C (gC m-2); (b) annual net N mineralization (gN yr-1 m-2); (c) annual NPP

(gC yr-1 m-2); (d) soil organic C (gC m-2); (e) soil moisture (% of total porosity); (f) soil temperature (°C); (g) Rh (gC yr-1 m-2); (h) NEP (gC yr-1 m-2).

Supplementary Files

This is a list of supplementary files associated with this preprint. Click to download.

- supplementalBZhaonc.docx